

Compromised epidermal barrier stimulates Harderian gland activity and hypertrophy in ACBP^{-/-} mice[§]

Signe Bek, Ditte Neess, Karen Dixen, Maria Bloksgaard,¹ Ann-Britt Marcher, John Chemnitz,¹ Nils J. Færgeman,² and Susanne Mandrup²

Department of Biochemistry and Molecular Biology, University of Southern Denmark, DK-5230 Odense M, Denmark

Abstract Acyl-CoA binding protein (ACBP) is a small, ubiquitously expressed intracellular protein that binds C₁₄–C₂₂ acyl-CoA esters with very high affinity and specificity. We have recently shown that targeted disruption of the *Acbp* gene leads to a compromised epidermal barrier and that this causes delayed adaptation to weaning, including the induction of the hepatic lipogenic and cholesterogenic gene programs. Here we show that ACBP is highly expressed in the Harderian gland, a gland that is located behind the eyeball of rodents and involved in the production of fur lipids and lipids used for lubrication of the eye lid. We show that disruption of the *Acbp* gene leads to a significant enlargement of this gland with hypertrophy of the acinar cells and increased de novo synthesis of monoalkyl diacylglycerol, the main lipid species produced by the gland. Mice with conditional targeting of the *Acbp* gene in the epidermis recapitulate this phenotype, whereas generation of an artificial epidermal barrier during gland development reverses the phenotype. Our findings indicate that the Harderian gland is activated by the compromised epidermal barrier as an adaptive and protective mechanism to overcome the barrier defect.—Bek, S., D. Neess, K. Dixen, M. Bloksgaard, A.-B. Marcher, J. Chemnitz, N. J. Færgeman, and S. Mandrup. Compromised epidermal barrier stimulates Harderian gland activity and hypertrophy in ACBP^{-/-} mice. *J. Lipid Res.* 2015. 56: 1738–1746.

Supplementary key words acyl-CoA binding protein • secretion • impaired epidermal barrier • monoalkyl diacylglycerol synthesis

The acyl-CoA binding protein (ACBP)/diazepam binding inhibitor, (entrez gene ID: 13167) is a 10kDa intracellular protein binding medium- and long-chain acyl-CoA ester (C₁₄–C₂₂) with high affinity and specificity (1). The protein is evolutionarily conserved and is expressed in all eukaryotic cell types investigated (2). However, expression levels differ markedly between different cell types. In general, lipogenic cell types as well as epithelial cells involved

in transport functions display high levels of ACBP expression, whereas heart, lung, muscle, and spleen have low expression levels (3–5). In vitro studies indicate that ACBP can act as an acyl-CoA pool former by protecting the acyl-CoA esters from hydrolysis (6, 7). In addition, ACBP relieves acyl-CoA inhibition of several enzymes in vitro (8–10). Depletion of the ACBP ortholog *Acb1* in *Saccharomyces cerevisiae* results in altered membrane structures, accumulation of vesicles, and compromised synthesis of very-long-chain fatty acids and sphingolipids (11, 12).

We recently generated mice with targeted disruption of the *Acbp* gene (ACBP^{-/-}) (13). These mice are born in a Mendelian ratio and are visually indistinguishable from their heterozygous and ACBP^{+/-} littermates until around 16 days of age, where the ACBP^{-/-} mice develop a matted and greasy fur. This fur phenotype persists throughout life and is at older age accompanied by scaling of the skin and occasional hair loss. Further investigations demonstrated that the epidermal barrier function is compromised in both young and adult ACBP^{-/-} mice (14), which, by analogy with other models (15–17), may be caused by the observed significant reduction of very-long-chain free fatty acids in the stratum corneum (14). Recently, we demonstrated that conditional targeting of the *Acbp* gene in keratinocytes of mice (K14-ACBP^{-/-}) recapitulates the defect epidermal barrier function, arguing that this defect is caused by lack of ACBP in the epidermis per se (18). In addition to the skin and hair phenotype, the ACBP^{-/-} mice suffer from a delayed adaptation to weaning, which includes a delayed hepatic upregulation of the lipogenic gene program at weaning (13). This is caused by suppression of the activity of the sterol-regulatory element binding proteins possibly as a result of increased hepatic accumulation

Abbreviations: ACBP, acyl-CoA binding protein; ACBP^{-/-}, mice with whole body ACBP depletion; HPTLC, high performance thin layer chromatography; K14-ACBP^{-/-}, mice with keratinocyte-specific ACBP depletion; MADAG, monoalkyl diacylglycerol; T3, triiodothyronine.

¹Current address: Institute of Molecular Medicine, University of Southern Denmark, J.B. Winsløvsvej 21, DK-5000 Odense C

²To whom correspondence should be addressed.

e-mail: s.mandrup@bmb.sdu.dk (S.M.); nils.f@bmb.sdu.dk (N.J.F.)

[§]The online version of this article (available at <http://www.jlr.org>) contains a supplement.

This work was supported by grants from the Danish Independent Research Council-Natural Science (S.M., N.J.F.) and from the Novo Nordisk Foundation (S.M., N.J.F.) The authors declare no conflicts of interest.

Manuscript received 20 May 2015 and in revised form 1 July 2015.

Published, JLR Papers in Press, July 4, 2015

DOI 10.1194/jlr.M060780

of triacylglycerol and cholesteryl esters (13). Intriguingly, we recently showed that *K14-ACBP*^{-/-} mice recapitulate the delayed hepatic adaptation to weaning, demonstrating that lack of ACBP in the epidermis leads to suppression of the lipogenic and cholesterogenic gene programs in the liver. Importantly, the hepatic phenotype could be rescued by establishing an artificial barrier using either Vaseline or latex, thereby for the first time establishing a physiological link between the epidermal barrier function and hepatic gene expression and metabolism (18).

The Harderian gland, originally discovered by Harder in 1694, is located behind the eyeball of most terrestrial vertebrates. The gland contains more than 20% lipids per wet weight, where neutral lipids constitute 55–57% of total lipids (19). The main lipid species in the murine Harderian gland is monoalkyl diacylglycerol (MADAG) (19, 20), which is secreted in an exocrine fashion onto the external surface of the cornea (21). Although the function(s) of the Harderian gland is still not completely understood, it is well established that lipids produced in the Harderian gland lubricate and protect the cornea and are used for grooming of the fur (22). In some species, lipids from the Harderian gland have been shown to provide thermoregulation (23–25). Thus, harderianectomy leads to a decrease in the ability of the muskrat and Mongolian gerbil to defend their core body temperature in cold water (23, 24). It was shown that the majority of the fur lipids originate from the Harderian gland in Mongolian gerbils; however, similar findings could not be observed in rats, hamsters, or mice (23). Thus, the function of the Harderian gland in thermo-protection in other rodents is unclear. In addition, the gland has been implicated in pheromone production and sexual behavior in some rodents (26–28).

Here we show that lack of ACBP in mice stimulates the activity and hypertrophy of the Harderian gland during weaning, and we present evidence indicating that this occurs as a defense mechanism in response to the impaired epidermal barrier of these mice.

MATERIALS AND METHODS

Generation and maintenance of mice

Generation of mice with constitutive (13) and conditional (18) targeting of the *Acbp* gene have previously been described. The mice were housed under standard conditions at ~55% relative humidity at 22 ± 3°C as described elsewhere (13). Cold exposure was carried out in a 4°C refrigerated room with normal light cycles and ad libitum access to food. Vaseline was applied as described previously (18). In brief, Vaseline was applied on the core body of the mice twice a day from 7 days of age to 28 days of age. The mice were weaned at 21 days of age as described (13). Breeding of transgenic mice and all animal experiments were approved by the Danish Animal Experiment Inspectorate.

Real-time PCR

For determination of mRNA levels, tissues were processed, and real-time PCR was carried out as previously described (13). Primers used are: *Acbp* fwd: 5' TTTGCGCATCCGTATCACCT; *Acbp* rev: 5'

TTTGCAAATTCAGCCTGAGACA; *Tfllb* fwd: 5' GTTCTGCTC-CAACCTTTGCGCT; *Tfllb* rev: 5' TGTGTAGCTGCCATCTGCACTT; *Adhaps* fwd: 5' TCCTATGGCTTGATGTGTCC; *Adhaps* rev: 5' GTCCTGTTATCCCAGCCTCT; *Dhapat* fwd: 5' GGTGTGTGTTGAATGAAGAAGG; *Dhapat* rev: 5' TGAAGGACAGCATGAGGAAG; *Acc* fwd: 5' AACTTGCCAGAGCAGAAGGCA; *Acc* rev: 5' GGATCTACCCAGGCCACATTG; *Fasn* fwd: 5' TGCCAGCGTGCAATGATG; *Fasn* rev: 5' CCTTTGAAGTCCAAGAAGAAGAGA.

Protein extraction, Western blotting, and ECL detection

Preparation of whole cell extracts, Western blotting, and ECL were carried out as described previously (13). Primary antibodies used were rabbit antiserum against ACBP (1:2,000) and rabbit anti-human TFIIB C-18 (1:1,000) (sc-225; Santa Cruz Biotechnology, Inc., Santa Cruz, CA). Secondary antibody used was HRP-conjugated swine anti-rabbit IgG (1:1,000) (Dako, Denmark).

Hematoxylin and eosin staining

Paraffin sections (5 μm) were mounted on Super Frost Plus[®] microscopic slides. Before staining, sections were dried for 60 min at 60°C, paraffin was removed with xylene, and sections were rehydrated with graded ethanol. Slides were then incubated in Mayer's hematoxylin (1 mg/ml in water) for 10 min and quickly in 1% HCl in 70% ethanol and rinsed for 10 min in flowing tap water before staining with eosin (2 min in 2% eosin in water). After staining, the slides were rinsed in water, dehydrated (2 × 1 min in 96% ethanol, 3 × 1 min in 99% ethanol, 2 × 5 min in xylene), and subsequently mounted.

Osmium tetroxide and toluidine blue staining

Adult mice were submitted to perfusion fixation with 2.5% glutaraldehyde in PBS (pH 7.4). Biopsies were postfixed in 1% osmium tetroxide (pH 7.2) for 2 h at 4°C, dehydrated in ethanol, and embedded in Araldite. Semithin sections (0.5 μm) were stained with toluidine blue for light microscopy.

Morphometry

The area of acinar cells, the number of vesicles per cell and per μm², and the diameter of the vesicles were measured in 0.5 μm sections stained with osmium tetroxide and toluidine blue using the Leica IM500 measurement application (100× magnification). Sections of glands from 3 month old *ACBP*^{-/-} (n = 6) and *ACBP*^{+/+} (n = 8) mice were evaluated. For each animal, the size and number of vesicles in a minimum of 10 acinar cells were determined.

De novo lipid synthesis and total lipid quantification in vivo

For determination of de novo lipid synthesis in the Harderian gland, adult mice (n = 8 for each genotype and condition) were injected i.p. with 0.04 μCi/g mouse ¹⁴C-acetic acid ([1-¹⁴C] acetic acid, sodium salt; Amersham Biosciences) in 0.9% saline and euthanized 1 h later by cervical dislocation. The Harderian glands were removed, snap-frozen in liquid nitrogen, and stored at -80°C. Total lipids were extracted from one Harderian gland using standard Bligh and Dyer extraction (29). Lipids from equal amounts of tissue were loaded onto silica plates (Merck High Performance Thin-Layer Chromatography [HPTLC]) and left to air dry for 15 min. The plates were developed in a horizontal development chamber in a solvent mixture of hexane-diethyl ether-acetic acid (v/v/v) (80:30:1) for the separation of neutral lipids. Band intensities were determined by densitometry. The visualization of ¹⁴C-labeled lipids and the total lipids was carried out as previously described (13).

Ex vivo secretion of de novo synthesized MADAG

Harderian glands were isolated from adult ACBP^{-/-} (n = 7) and ACBP^{+/+} (n = 7) mice and washed in Krebs ringer buffer (Sigma) containing 0.5% fatty acid-free BSA (Sigma). Immediately thereafter, similar-sized explants (approximately half a gland) were incubated for 2 h in Krebs ringer buffer with 1% fatty acid-free BSA containing 0.5 μ Ci/ml ¹⁴C-acetic acid ([1-¹⁴C] acetic acid, sodium salt; Amersham Biosciences) at 37°C. Explants were removed and washed, and the weight was determined. Lipids were extracted from the media as described above. The extracted lipids were diluted relative to the explant weight (equal volume per tissue weight) and analyzed by HPTLC as described above.

Choline level in the Harderian gland

The free level of choline in the Harderian gland was measured using a Choline/Acetylcholine Quantification Kit (MAK056-1KT; Sigma). Harderian glands from adult mice were homogenized in supplied assay buffer, and the level of choline was determined according to the manufacturer by fluorometry using a FLOUstar Omega fluorescence plate reader (BMG Labtech) and normalized to protein content as determined by a PierceTM BCA Protein Assay kit (23227; Thermo Scientific).

Plasma triiodothyronine

Plasma from fed adult mice were collected and separated as described elsewhere (13). The triiodothyronine (T3) level was analyzed using a FLOUstar Omega fluorescence plate reader (BMG Labtech) and a mouse/rat T3 ELISA kit (T3043T-100, Calbiotech).

RESULTS

ACBP is expressed at a high level in the Harderian gland

ACBP^{-/-} mice consistently display swollen eyelids and increased secretion from the eye cavity (Fig. 1A). This phenotype is visible from around weaning and persists throughout adulthood. Interestingly, when we examined the eye cavity of adult mice, we found that the lipid-producing Harderian gland is approximately twice as large in ACBP^{-/-} mice compared with ACBP^{+/+} mice (Fig. 1B). Examination of the expression of ACBP in this gland showed that, similar to other lipogenic tissues (Fig. 1E) (4, 30, 31), ACBP is expressed at very high levels in Harderian gland of ACBP^{+/+} mice. In contrast, ACBP is completely absent in the Harderian gland of ACBP^{-/-} mice (Fig. 1C, D).

In mice, the Harderian gland is not fully developed at birth. It becomes functional from around 14 days of age when the pups open their eyes; however, the gland continues to grow and mature until adulthood (32). We found that the size of the gland is similar in ACBP^{-/-} and ACBP^{+/+} mice until just before weaning at 21 days of age (Fig. 1F). However, in the week after weaning, the size of the Harderian glands of ACBP^{-/-} mice doubles, whereas gland size in ACBP^{+/+} mice remains relatively constant. This is true both when gland size is normalized to body weight (Fig. 1F) and when it is expressed only as gland weight (supplementary Fig. 1). This indicates that weaning initiates systemic and/or endogenous signals in the gland that leads to a major and rapid hypertrophy of the gland, which is maintained in adulthood.

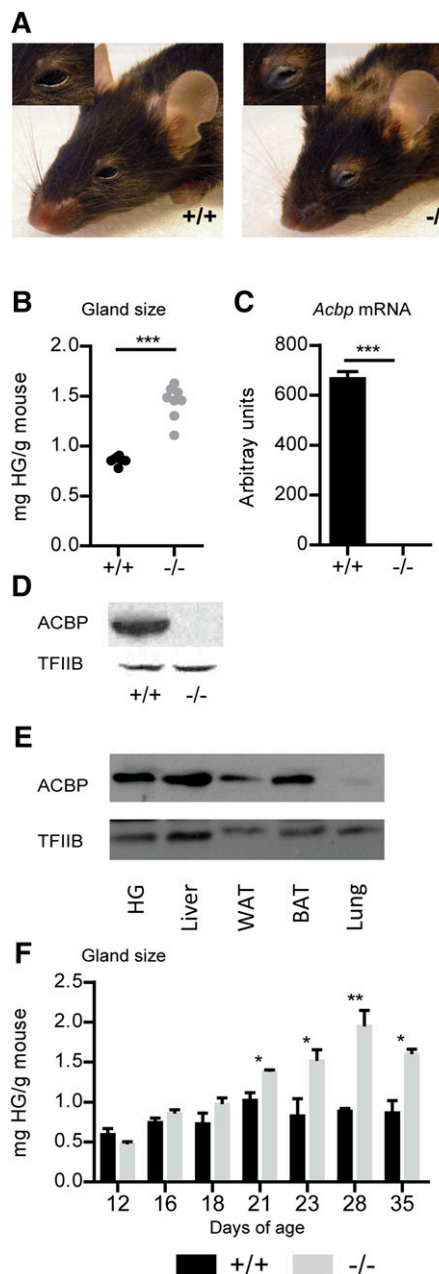


Fig. 1. Harderian gland size is increased in ACBP^{-/-} mice. A: ACBP^{-/-} mice display swollen eyelids and increased secretion from the eye cavity. B: Weight of Harderian glands from 3 month old ACBP^{-/-} and ACBP^{+/+} male mice (n = 8). Data are presented as mg Harderian gland per gram mouse. *** $P < 0.001$. Expression of ACBP mRNA (C) and protein (D) in the Harderian glands from 3 month old ACBP^{-/-} and ACBP^{+/+} male mice. RNA was quantified using real-time PCR (n = 8). Error bars represent SEM. *** $P < 0.001$. Protein expression was visualized by Western blotting of protein extracts pooled from five animals. E: Comparison of ACBP expression in Harderian glands relative to other tissues with high expression of ACBP. ACBP expression was visualized by Western blotting of protein extract (pooled from four mice). F: Harderian glands are enlarged in ACBP^{-/-} mice from weaning at 21 days of age. Harderian glands were isolated from mice (n = 3) at the indicated age, and the weight was determined and normalized to bodyweight. Error bars indicate mean \pm SEM. * $P < 0.05$; ** $P < 0.01$. Significance was determined using unpaired parametric Student's *t*-test. BAT, brown adipose tissue; HG, Harderian gland; WAT, white adipose tissue (inguinal).

The Harderian gland consists of a simple tubuloalveolar system with acinar cells arranged in acini (33). This overall structure is maintained in the ACBP^{-/-} mice (Fig. 2A); however, the acinar cells from ACBP^{-/-} mice are larger (Fig. 2C) and contain fewer (Fig. 2A, E, F) but significantly larger vesicles (Fig. 2D) compared with glands from ACBP^{+/+} mice. Furthermore, lipid staining with osmium tetroxide demonstrated that the vesicles and the lumen contained more lipid in the ACBP^{-/-} glands compared with ACBP^{+/+} glands (Fig. 2B). These data indicate that lack of ACBP causes hypertrophy and increased activity of the Harderian gland.

Depletion of ACBP leads to increased secretion of MADAG from the Harderian gland

The increased size and lipid filling of the vesicles in the Harderian gland of ACBP^{-/-} mice prompted us to investigate the lipid content of the gland. We therefore carefully dissected the gland and extracted the lipids. Using HPTLC, we found that the major overall change in lipid classes was

a decrease in the amount of MADAG, the main lipid product of the Harderian gland (19, 20), in glands from ACBP^{-/-} mice compared with the glands from ACBP^{+/+} mice (Fig. 3A and data not shown). The fatty acids used for synthesis of MADAG originate primarily from de novo fatty acid synthesis in the gland (34, 35). In vivo pulse-labeling with ¹⁴C-acetic acid showed that de novo synthesis of MADAG in Harderian glands is significantly higher in ACBP^{-/-} mice compared with ACBP^{+/+} mice (Fig. 3B). However, this increase occurred in the absence of changes in the mRNA expression of key enzymes involved in synthesis of MADAG (35), such as dihydroxyacetone phosphate acyltransferase 1-alkyl-dihydroxyacetone phosphate synthase (supplementary Fig. 2A, B). Similarly, there was no increase in the expression of genes encoding key enzymes in the synthesis of fatty acids, such as fatty acid synthase or acetyl-CoA carboxylase (supplementary Fig. 2C, D). This indicates that the increase in the synthesis of MADAG is not driven by increased expression of enzymes involved in synthesis of fatty acids but rather by increased activity of

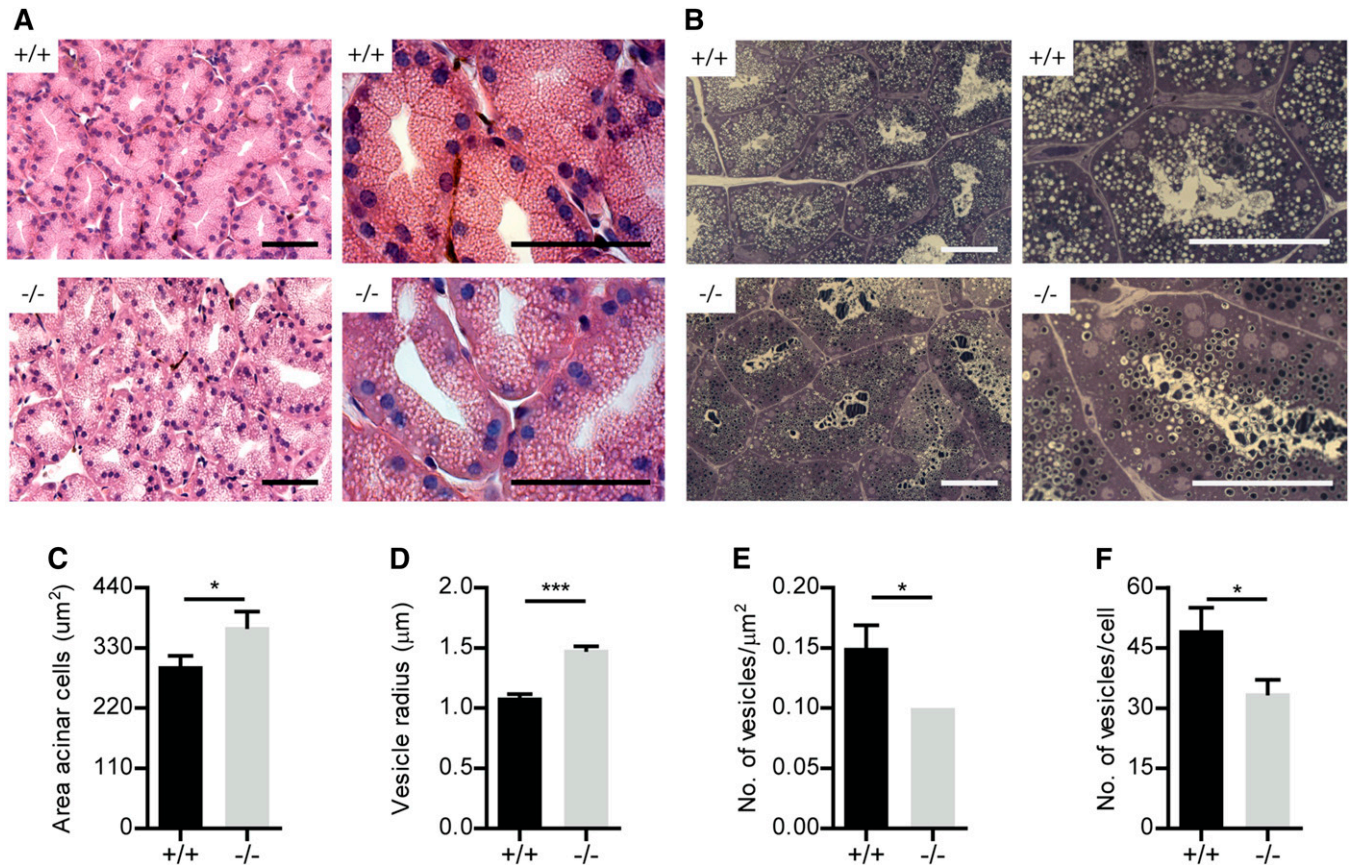


Fig. 2. Depletion of ACBP results in altered morphology of the Harderian gland. A: Staining with hematoxylin and eosin revealing the overall Harderian gland morphology in the ACBP^{+/+} and ACBP^{-/-} mice. The sections shown are representative of at least five sections of the Harderian gland of three ACBP^{-/-} and three ACBP^{+/+} adult male mice, respectively. The scale bars represent 50 µm. B: Lipid staining using osmium tetroxide and toluidine blue reveals the increased lipid filling of the gland lumen in the ACBP^{-/-} mice. The images are representative of at least three sections from four animals per genotype. The scale bars represent 50 µm. Stereological investigations of the OsO₄-stained sections revealed an increased cell size (C) with an increased size of vesicles (D), a decreased number of vesicles per µm² (E), and a decreased number of vesicles per cell (F) in the Harderian gland from ACBP^{-/-} mice (n = 6) compared with glands from ACBP^{+/+} mice (n = 8). For each mouse, at least 10 cells and 10 vesicles/cell were measured. Data are presented as mean ± SEM. * *P* < 0.05; *** *P* < 0.001. Significance was determined using unpaired parametric Student's *t*-test.

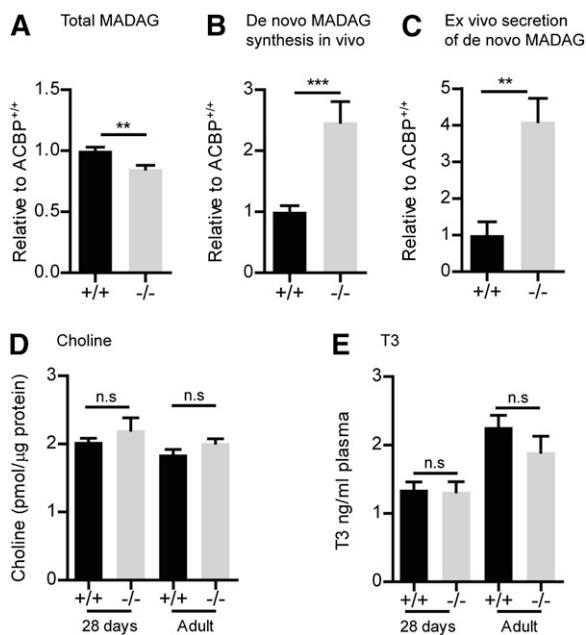


Fig. 3. De novo MADAG synthesis is increased in the Harderian gland of ACBP^{-/-} mice. **A:** Total MADAG per weight tissue in Harderian glands of ACBP^{+/+} and ACBP^{-/-} mice ($n = 8$ per genotype). Lipids were extracted from similar amounts of Harderian glands, and samples were diluted to obtain equal volume per tissue weight in all samples. Neutral lipids were analyzed by HPTLC, and total MADAG was determined by densitometry and plotted relative to the ACBP^{+/+} levels. Data are presented as mean \pm SEM. ****** $P < 0.01$. **B:** De novo synthesis of MADAG in adult male mice ($n = 8$ per genotype) was determined by in vivo pulse-labeling with ¹⁴C-acetic acid for 2 h. Lipids were extracted from similar amounts of Harderian gland, and samples were diluted to obtain equal volume per tissue weight. De novo MADAG synthesis was determined by quantification of radioactivity in MADAG bands and expressed relative to the mean value in Harderian glands of ACBP^{+/+} mice. Data are presented as mean \pm SEM. ******* $P < 0.001$. **C:** Secretion of de novo synthesized MADAG from Harderian gland explants from adult male mice ($n = 7$ per genotype) was determined by ex vivo pulse-labeling with ¹⁴C-acetic acid for 2 h. Lipid were extracted from the media and quantified by HPTLC as above. MADAG secretion from Harderian gland explants is expressed relative to the mean normalized secretion from ACBP^{+/+} explants. Data are presented as mean \pm SEM. ****** $P < 0.01$. **D:** The level of choline in the Harderian glands was determined in adult ($n = 9$) and 28 day old ($n = 5-6$) ACBP^{+/+} and ACBP^{-/-} mice. Data are presented as mean \pm SEM. **E:** Plasma T3 levels were determined in plasma from adult ($n = 7$) and 28 day old ($n = 5-6$) ACBP^{+/+} and ACBP^{-/-} mice. Data are presented as mean \pm SEM. Significance was determined using unpaired parametric Student's *t*-test (n.s., nonsignificant).

these enzymes and/or increased substrate flux. Choline and T3 have been shown to stimulate secretion from the Harderian gland in rats (36–40). However, neither plasma levels of T3 nor glandular choline levels were affected by ACBP depletion at 28 days of age or in adult mice (Fig. 3D, E). This indicates that the observed increase in Harderian gland activity in ACBP-depleted mice is not caused by changes in choline or T3 levels.

Taken together, these data show that the enlarged Harderian glands in ACBP^{-/-} mice synthesize more MADAG per weight gland compared with glands from ACBP^{+/+} mice. Despite this, the total MADAG content of

the gland is lower in ACBP^{-/-} mice than in ACBP^{+/+} mice, suggesting that secretion of MADAG from the gland exceeds the increase in synthesis rate. To further investigate this, we isolated Harderian glands and exposed similar-sized explants to 2 h ex vivo pulse-labeling with ¹⁴C-acetic acid. Analysis of the explant medium showed that secretion of MADAG is significantly higher for ACBP^{-/-} compared with ACBP^{+/+} explants (Fig. 3C).

The effect of thermoregulation on the activity of the Harderian glands

We have previously shown that ACBP^{-/-} pups tolerate weaning less well and need to be housed with littermates and soaked food in the bottom of the cage to survive (13). We therefore speculated that the hypertrophy and increased activity of the Harderian gland may be caused by cold perception. To investigate whether cold exposure per se could induce Harderian gland activity, we exposed adult ACBP^{+/+} mice to cold (4°C) for 15 days. Interestingly, this resulted in a modest but significant increase in Harderian gland size (Fig. 4A) and in a reduction in total MADAG level (Fig. 4B) when compared with Harderian glands of ACBP^{+/+} mice kept at room temperature. However, de novo MADAG synthesis, as determined by in vivo pulse-labeling with ¹⁴C-acetic acid, was not affected by cold exposure (Fig. 4C). This indicates that cold perception can indeed lead to an increase in gland size but that the increase in size and activity is much less dramatic than what is observed in the ACBP^{-/-} mice around weaning.

Endogenous effects of ACBP depletion on the Harderian gland

We recently reported that mice with conditional targeting of the *Acbp* gene in keratinocytes (K14-ACBP^{-/-}), similar to ACBP^{-/-} mice, display a compromised epidermal barrier and an increased transepidermal water loss (14, 18). Furthermore, the K14-ACBP^{-/-} mice recapitulate the delayed hepatic adaption during weaning previously observed in ACBP^{-/-} mice (13, 18). Importantly, we were able to rescue the hepatic phenotype by creating an artificial epidermal barrier using Vaseline or latex, thereby demonstrating that it is the impaired barrier per se, possibly through an increased heat loss, that leads to changes in hepatic gene expression and metabolism during weaning.

To investigate if the imperfect epidermal barrier may also cause Harderian gland hypertrophy and increased activity at weaning, we took advantage of the K14-ACBP^{-/-} mice (18). Careful examination of the K14-ACBP^{-/-} mice revealed that ACBP was not only depleted in the keratinocytes but also in the Harderian glands (Fig. 5A, B). This is consistent with a previous report from Ntambi and coworkers reporting that the K14 promoter drives CRE-mediated disruption of the *Scd1* locus in the Harderian gland in addition to the epidermis (41). Interestingly, examination of Harderian glands from K14-ACBP^{-/-} mice revealed that these are also significantly larger than those from control mice (Fig. 5C). Furthermore, similar to Harderian glands from ACBP^{-/-} mice, glands from K14-ACBP^{-/-}

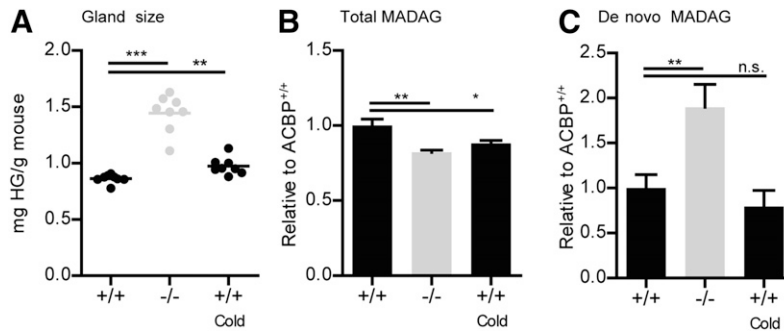


Fig. 4. Cold exposure for 15 days leads to a modest increase in the size of the Harderian gland of adult mice. Harderian glands of male ACBP^{+/+} mice maintained in standard housing conditions (22°C) or exposed to cold (4°C) for 15 days were compared with Harderian glands of male ACBP^{-/-} mice maintained in standard housing conditions. **A:** Weight of the Harderian glands of adult mice (n = 8 per genotype and condition). Data are presented as mg Harderian glands per gram mouse. ** *P* < 0.01; *** *P* < 0.001. **B:** Total MADAG per weight tissue in Harderian glands of mice (n = 4–7 per genotype and condition) was determined by HPTLC. Lipids were extracted, and samples were diluted to obtain equal volume per tissue weight in all samples. Total MADAG per weight tissue was determined by densitometry and plotted relative to the mean level in Harderian glands of ACBP^{+/+} mice maintained in standard housing conditions. Data are presented as mean ± SEM. * *P* < 0.05; ** *P* < 0.01. **C:** De novo synthesis of MADAG in Harderian glands of adult male mice (n = 4–7) was determined by in vivo pulse-labeling with ¹⁴C-acetic acid. Lipids were extracted from Harderian glands, and samples were diluted to obtain equal volume per tissue weight in all samples. De novo MADAG synthesis was determined by quantification of radioactivity in MADAG bands and expressed relative to the mean value in Harderian glands of ACBP^{+/+} mice maintained in standard housing conditions. Data are presented as mean ± SEM. ** *P* < 0.01. Significance was determined using unpaired parametric Student's *t*-test (n.s., nonsignificant).

mice contain lower levels of MADAG (Fig. 5D) and display a significantly increased de novo synthesis of MADAG (Fig. 5E). Collectively, these data indicate that the phenotype of the Harderian gland in ACBP^{-/-} mice is caused primarily by the lack of ACBP in the epidermis and/or in the Harderian gland itself.

Impairment of the epidermal barrier activates the Harderian gland

To investigate whether the impaired epidermal barrier in ACBP^{-/-} and K14-ACBP^{-/-} mice was causally related to the phenotype of the Harderian gland, we examined the effect of Vaseline on gland size. Vaseline was applied to the core body of the mice twice a day from 7 to 28 days of age to generate an artificial epidermal barrier during the time when the glands of ACBP^{-/-} mice experience the most dramatic increase in gland size (Fig. 1F). Interestingly, Vaseline occlusion of the epidermis eliminates the size difference between Harderian glands from 28 day old ACBP^{+/+} and ACBP^{-/-} mice (Fig. 6A), indicating that it is the compromised epidermal barrier that stimulates the hypertrophy of the gland in ACBP^{-/-} mice around weaning. Importantly, Vaseline also normalizes total MADAG content (Fig. 6B) and de novo synthesis of MADAG in these mice (Fig. 6C).

These results show for the first time that an impaired epidermal barrier can stimulate hypertrophy and activity of the Harderian gland and flux of MADAG from the Harderian gland. The exact signaling pathways and molecular mechanisms underlying this dramatic effect on the gland remains unclear; however, it is likely that water and/or heat loss across the epidermis initiates a protective systemic

response that stimulates the gland to enlarge and to produce more protective lipid for secretion on the fur. Consistent with that, we have shown that there is significantly more total lipid, including MADAG, on the fur of ACBP^{-/-} mice than on the fur of ACBP^{+/+} mice (14).

DISCUSSION

In this study, we show that targeted disruption of ACBP leads to hypertrophy and increased activity of the Harderian gland, and we demonstrate that this occurs as a result of the impaired epidermal barrier of the ACBP^{-/-} mice. The hypertrophy of the Harderian gland is induced around and immediately subsequent to weaning, indicating that it occurs as a result of the challenges faced by the ACBP^{-/-} mice at weaning.

Morphometric measurements indicated that the increased gland size found in the ACBP^{-/-} Harderian gland is the result of marked hypertrophy and possibly also of modest hyperplasia of the acinar cells. Furthermore, there are several indications that ACBP^{-/-} glands are more active and secrete more lipids. First, although total content of MADAG was decreased in glands from ACBP^{-/-} mice, we show that there is a significant increase in the de novo synthesis of MADAG in these glands. Second, vesicles in ACBP^{-/-} glands are larger and contain more lipids compared with vesicles in ACBP^{+/+} mice, a phenomenon also observed in choline-stimulated Harderian glands (21, 39, 40). An estimate of the percentage of the gland volume taken up by vesicles indicates that the relative vesicle volume is slightly increased in glands from ACBP^{-/-} mice relative to ACBP^{+/+} mice. It is possible that MADAG is more

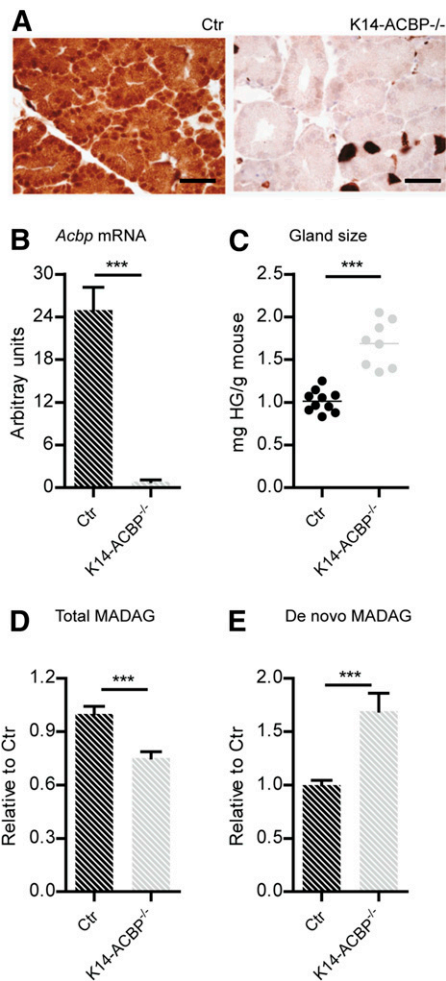


Fig. 5. Harderian glands of K14-ACBP^{-/-} mice phenocopy Harderian glands of ACBP^{-/-} mice. **A:** Immunohistochemical detection of ACBP in the Harderian glands of heterozygote control mice and K14-ACBP^{-/-} mice. Sections are representative of three adult males of each genotype. The scale bar represents 50 μ m. **B:** Expression of *Acbp* mRNA in the Harderian glands of adult male control and K14-ACBP^{-/-} mice. RNA expression was quantified using real-time PCR ($n = 8$). Data represent mean \pm SEM. *** $P < 0.001$. **C:** Weight of the Harderian glands of adult control mice ($n = 10$) and K14-ACBP^{-/-} mice ($n = 8$). Data are presented as mg Harderian gland per gram mouse. *** $P < 0.001$. **D:** Total MADAG in Harderian glands of control ($n = 6$) and K14-ACBP^{-/-} mice ($n = 5$) was determined by HPTLC. Lipids were extracted, and samples were diluted to obtain equal volume per tissue weight in all samples. Total MADAG per weight tissue was determined by densitometry and plotted relative to the mean level in Harderian glands of control mice. Data are presented as mean \pm SEM. *** $P < 0.001$. **E:** De novo synthesis of MADAG in the Harderian glands of adult male control ($n = 6$) and K14-ACBP^{-/-} ($n = 5$) mice as determined by in vivo pulse-labeling with ¹⁴C-acetic acid. Lipids were extracted from Harderian glands, and samples were diluted to obtain equal volume per tissue weight in all samples. De novo MADAG synthesis was determined by quantification of radioactivity in MADAG bands and expressed relative to the mean value in Harderian glands of control mice. De novo MADAG synthesis is displayed relative to mean values in control mice. Data are presented as mean \pm SEM. *** $P < 0.01$. Significance was determined using unpaired parametric Student's *t*-test.

rapidly packaged into vesicles in ACBP^{-/-} mice. Third, we have previously shown that there is three times more MADAG on the fur of ACBP^{-/-} mice compared with that

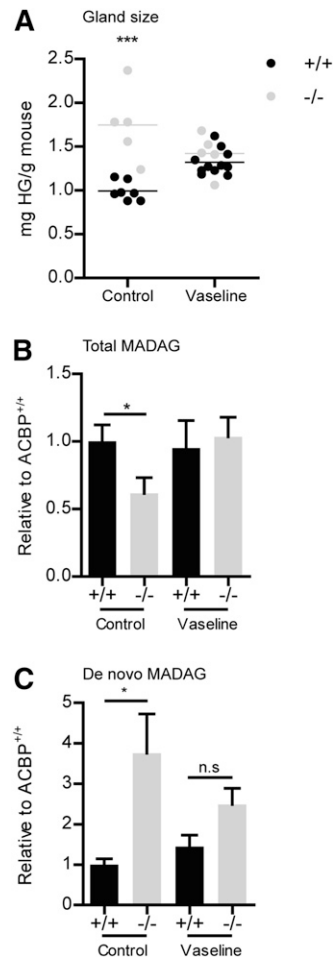


Fig. 6. Establishment of an artificial epidermal barrier rescues the phenotype of the Harderian glands in ACBP^{-/-} mice. Vaseline was applied twice a day from 7 to 28 days of age on the entire body of ACBP^{-/-} ($n = 5$) and ACBP^{+/+} mice ($n = 11$). **A:** Relative weight of Harderian glands from 28 day old control or Vaseline-treated ACBP^{+/+} ($n = 11$) and ACBP^{-/-} ($n = 5$) mice. Data are presented as mg Harderian gland per gram mouse. *** $P < 0.001$. **B:** Total MADAG per weight tissue in weight tissue in Harderian glands of 28 day old control or Vaseline-treated ACBP^{+/+} and ACBP^{-/-} ($n = 5$). Lipids were extracted, and samples were diluted to obtain equal volume per tissue weight in all samples. Total MADAG per weight tissue was determined by densitometry and plotted relative to the mean level in Harderian glands of control ACBP^{+/+} mice. Data are presented as mean \pm SEM. * $P < 0.05$. **C:** De novo synthesis of MADAG per weight Harderian gland in 28 day old control or Vaseline-treated ACBP^{-/-} and ACBP^{+/+} mice ($n = 5$) was determined by pulse-labeling with ¹⁴C-acetic acid. Lipids were extracted from Harderian glands, and samples were diluted to obtain equal volume per tissue weight in all samples. De novo MADAG synthesis was determined by quantification of radioactivity in MADAG bands and expressed relative to the mean value in Harderian glands of control ACBP^{+/+} mice. Data are presented as mean \pm SEM. * $P < 0.05$. Significance was determined using unpaired parametric Student's *t*-test.


of ACBP^{+/+} mice (14). Finally, we show that glandular explants from ACBP^{-/-} mice secrete significantly more MADAG than explants from ACBP^{+/+} mice. Taken together, these findings strongly indicate that Harderian glands from ACBP^{-/-} mice are not only larger but also more active than glands from ACBP^{+/+} mice. Thus, although the

relative contribution of lipids from the Harderian gland to fur lipid in mice is unclear (23, 42), our results indicate that stimulation of the Harderian gland could indeed contribute to fur lipids.

We show that, similar to other lipogenic cells (4, 5, 30, 31, 43), the acinar cells of the Harderian gland express very high levels of ACBP. We therefore initially speculated that the Harderian gland phenotype was caused directly by failure to express ACBP in these cells. This hypothesis was consistent with the finding that the K14 promoter is also active in the acinar cells and that K14-ACBP^{-/-} mice recapitulate the Harderian gland phenotype. Importantly, however, the Harderian gland phenotype with increased gland size and activity could be rescued by Vaseline occlusion of the epidermis before and during weaning. Thus, although we cannot exclude a contribution from endogenous lack of ACBP in the Harderian gland, our results show for the first time that hypertrophy and increased activity of the Harderian gland is caused primarily by the compromised epidermal barrier.

It is currently unclear how the imperfect barrier signals to the Harderian gland to increase activity. Adrenergic nerve fibers and cholinergic fibers are associated with blood vessels and secretory and myoepithelial cells in the murine Harderian gland, respectively (44). Increased levels of both choline and the thyroid hormone T3 has been shown to lead to increased lipid secretion from the Harderian gland in rats (21, 36, 39). However, ACBP^{-/-} mice neither presented increased glandular levels of choline nor increased plasma levels of T3 (Fig. 3D, E), indicating that these pathways are not responsible for the increased activity of the gland in ACBP^{-/-} mice. Thus, it appears that the epidermis signals to promote gland activity and hypertrophy through alternative mechanisms.

Whatever the signals are, our results indicate that the potential to induce gland hypertrophy and activity is greater in the days after weaning compared with in adult mice where prolonged cold exposure only led to a minor increase in gland size but no increase in de novo MADAG synthesis. A possible reason for this could be that the Harderian gland is more sensitive to activating signals in pups than in adult mice. Alternatively, ACBP^{-/-} and K14-ACBP^{-/-} pups perceive a stronger cold signal at room temperature than adult ACBP^{+/+} mice do at 4°C.

In conclusion, we have demonstrated that the Harderian gland of ACBP^{-/-} mice displays significant hypertrophy and increased activity, which is instigated around weaning and is caused by the impaired epidermal barrier of these mice. This represents the first direct demonstration that impairment of the epidermal barrier can stimulate the activity of this gland. We propose that this occurs as a protective mechanism, in particular in pups, to increase the production of fur lipids and thereby overcome the barrier defect. 

The authors thank laboratory technicians Yoanna Vladimirova and Brigita Meskauskaitė for technical assistance.

REFERENCES

- Rosendal, J., P. Ertbjerg, and J. Knudsen. 1993. Characterization of ligand binding to acyl-CoA-binding protein. *Biochem. J.* **290**: 321–326.
- Burton, M., T. M. Rose, N. J. Faergeman, and J. Knudsen. 2005. Evolution of the acyl-CoA binding protein (ACBP). *Biochem. J.* **392**: 299–307.
- Bovolin, P., J. Schlichting, M. Miyata, C. Ferrarese, A. Guidotti, and H. Alho. 1990. Distribution and characterization of diazepam binding inhibitor (DBI) in peripheral tissues of rat. *Regul. Pept.* **29**: 267–281.
- Neess, D., P. Kiellerich, M. B. Sandberg, T. Helledie, R. Nielsen, and S. Mandrup. 2006. ACBP: a PPAR and SREBP modulated housekeeping gene. *Mol. Cell. Biochem.* **284**: 149–157.
- Hansen, H. O., P. H. Andreassen, S. Mandrup, K. Kristiansen, and J. Knudsen. 1991. Induction of acyl-CoA-binding protein and its mRNA in 3T3-L1 cells by insulin during preadipocyte-to-adipocyte differentiation. *Biochem. J.* **277**: 341–344.
- Knudsen, J., N. J. Faergeman, H. Skott, R. Hummel, C. Borsting, T. M. Rose, J. S. Andersen, P. Hojrup, P. Roepstorff, and K. Kristiansen. 1994. Yeast acyl-CoA-binding protein: acyl-CoA-binding affinity and effect on intracellular acyl-CoA pool size. *Biochem. J.* **302**: 479–485.
- Mandrup, S., R. Jepsen, H. Skott, J. Rosendal, P. Hojrup, K. Kristiansen, and J. Knudsen. 1993. Effect of heterologous expression of acyl-CoA-binding protein on acyl-CoA level and composition in yeast. *Biochem. J.* **290**: 369–374.
- Chao, H., M. Zhou, A. McIntosh, F. Schroeder, and A. B. Kier. 2003. ACBP and cholesterol differentially alter fatty acyl CoA utilization by microsomal ACAT. *J. Lipid Res.* **44**: 72–83.
- Mogensen, I. B., H. Schulenberg, H. O. Hansen, F. Spener, and J. Knudsen. 1987. A novel acyl-CoA-binding protein from bovine liver. Effect on fatty acid synthesis. *Biochem. J.* **241**: 189–192.
- Rasmussen, J. T., J. Rosendal, and J. Knudsen. 1993. Interaction of acyl-CoA binding protein (ACBP) on processes for which acyl-CoA is a substrate, product or inhibitor. *Biochem. J.* **292**: 907–913.
- Faergeman, N. J., S. Feddersen, J. K. Kristiansen, M. K. Larsen, R. Schneider, C. Ungerermann, K. Mutenda, P. Roepstorff, and J. Knudsen. 2004. Acyl-CoA-binding protein, Acblp, is required for normal vacuole function and ceramide synthesis in *Saccharomyces cerevisiae*. *Biochem. J.* **380**: 907–918.
- Gaigg, B., T. B. Neergaard, R. Schneider, J. K. Hansen, N. J. Faergeman, N. A. Jensen, J. R. Andersen, J. Friis, R. Sandhoff, H. D. Schroder, et al. 2001. Depletion of acyl-coenzyme A-binding protein affects sphingolipid synthesis and causes vesicle accumulation and membrane defects in *Saccharomyces cerevisiae*. *Mol. Biol. Cell.* **12**: 1147–1160.
- Neess, D., M. Bloksgaard, S. Bek, A. B. Marcher, I. C. Elle, T. Helledie, M. Due, V. Pagmantidis, B. Finsen, J. Wilbertz, et al. 2011. Disruption of the acyl-CoA-binding protein gene delays hepatic adaptation to metabolic changes at weaning. *J. Biol. Chem.* **286**: 3460–3472.
- Bloksgaard, M., S. Bek, A. B. Marcher, D. Neess, J. Brewer, H. K. Hannibal-Bach, T. Helledie, C. Fenger, M. Due, Z. Berzina, et al. 2012. The acyl-CoA binding protein is required for normal epidermal barrier function in mice. *J. Lipid Res.* **53**: 2162–2174.
- Li, W., R. Sandhoff, M. Kono, P. Zerfas, V. Hoffmann, B. C. Ding, R. L. Proia, and C. X. Deng. 2007. Depletion of ceramides with very long chain fatty acids causes defective skin permeability barrier function, and neonatal lethality in ELOVL4 deficient mice. *Int. J. Biol. Sci.* **3**: 120–128.
- Miyazaki, M., A. Dobrzyn, P. M. Elias, and J. M. Ntambi. 2005. Stearoyl-CoA desaturase-2 gene expression is required for lipid synthesis during early skin and liver development. *Proc. Natl. Acad. Sci. USA.* **102**: 12501–12506.
- Stone, S. J., H. M. Myers, S. M. Watkins, B. E. Brown, K. R. Feingold, P. M. Elias, and R. V. Farese, Jr. 2004. Lipopenia and skin barrier abnormalities in DGAT2-deficient mice. *J. Biol. Chem.* **279**: 11767–11776.
- Neess, D., S. Bek, M. Bloksgaard, A. B. Marcher, N. J. Faergeman, and S. Mandrup. 2013. Delayed hepatic adaptation to weaning in ACBP^{-/-} mice is caused by disruption of the epidermal barrier. *Cell Reports.* **5**: 1403–1412.
- Tvrzicka, E., T. Rezanka, J. Krijt, and V. Janousek. 1988. Identification of very-long-chain fatty acids in rat and mouse harderian gland lipids by capillary gas chromatography-mass spectrometry. *J. Chromatogr. A.* **431**: 231–238.

20. Kasama, K., M. L. Blank, and F. Snyder. 1989. Identification of 1-alkyl-2-acyl-3-(2',3'-diacylglycerol)glycerols, a new type of lipid class, in harderian gland tumors of mice. *J. Biol. Chem.* **264**: 9453–9461.
21. Satoh, Y., A. P. Gesase, Y. Habara, K. Ono, and T. Kanno. 1996. Lipid secretory mechanisms in the mammalian harderian gland. *Microsc. Res. Tech.* **34**: 104–110.
22. Cohn, S. A. 1955. Histochemical observations on the Harderian gland of the albino mouse. *J. Histochem. Cytochem.* **3**: 342–353.
23. Thiessen, D. D., and E. M. Kittrell. 1980. The Harderian gland and thermoregulation in the gerbil (*Meriones unguiculatus*). *Physiol. Behav.* **24**: 417–424.
24. Harlow, H. J. 1984. The Influence of Harderian gland removal and fur lipid removal on heat loss, and water flux to and from the skin of muskrats, *Ondatra zibethicus*. *Physiol. Zool.* **57**: 349–356.
25. Shanas, U., and J. Terkel. 1996. Grooming secretions and seasonal adaptations in the blind mole rat (*Spalax ehrenbergi*). *Physiol. Behav.* **60**: 653–656.
26. Thiessen, D. D., and A. E. Harriman. 1986. Harderian gland exudates in the male *Meriones unguiculatus* regulate female proceptive behavior, aggression, and investigation. *J. Comp. Psychol.* **100**: 85–87.
27. Payne, A. P. 1979. The attractiveness of Harderian gland smears to sexually naive and experienced male golden hamsters. *Anim. Behav.* **27**: 897–904.
28. Payne, A. P. 1977. Pheromonal effects of Harderian gland homogenates on aggressive behaviour in the hamster. *J. Endocrinol.* **73**: 191–192.
29. Bligh, E. G., and W. J. Dyer. 1959. A rapid method of total lipid extraction and purification. *Can. J. Biochem. Physiol.* **37**: 911–917.
30. Alho, H., R. T. Fremereau, Jr., H. Tiedge, J. Wilcox, P. Bovolin, J. Brosius, J. L. Roberts, and E. Costa. 1988. Diazepam binding inhibitor gene expression: location in brain and peripheral tissues of rat. *Proc. Natl. Acad. Sci. USA.* **85**: 7018–7022.
31. Alho, H., T. Harjuntausta, R. Schultz, M. Peltto-Huikko, and P. Bovolin. 1991. Immunohistochemistry of diazepam binding inhibitor (DBI) in the central nervous system and peripheral organs: its possible role as an endogenous regulator of different types of benzodiazepine receptors. *Neuropharmacology.* **30**: 1381–1386.
32. Shirama, K., and M. Hokano. 1991. Electron-microscopic studies on the maturation of secretory cells in the mouse Harderian gland. *Acta Anat. (Basel).* **140**: 304–312.
33. Shirama, K., and M. Hokano. 1992. Harderian glands and their development in laboratory rats and Mice. In *Harderian Glands*. S. Webb, R. Hoffman, M. Puig-Domingo, and R. Reiter, editors. Springer Berlin Heidelberg. 25–51.
34. Miyazaki, M., H. J. Kim, W. C. Man, and J. M. Ntambi. 2001. Oleoyl-CoA is the major de novo product of stearoyl-CoA desaturase 1 gene isoform and substrate for the biosynthesis of the Harderian gland 1-alkyl-2,3-diacylglycerol. *J. Biol. Chem.* **276**: 39455–39461.
35. Seyama, Y., T. Kasama, E. Yasugi, S-H. Park, and K. Kano. 1992. Lipids in Harderian Glands and Their Significance. In *Harderian Glands*. S. Webb, R. Hoffman, M. Puig-Domingo, and R. Reiter, editors. Springer, Berlin, Heidelberg. 195–217.
36. Chieffi Baccari, G., R. Monteforte, P. de Lange, F. Raucci, P. Farina, and A. Lanni. 2004. Thyroid hormone affects secretory activity and uncoupling protein-3 expression in rat harderian gland. *Endocrinology.* **145**: 3338–3345.
37. Monteforte, R., A. Santillo, A. Lanni, S. D'Aniello, and G. C. Baccari. 2008. Morphological and biochemical changes in the Harderian gland of hypothyroid rats. *J. Exp. Biol.* **211**: 606–612.
38. Satoh, Y., Y. Habara, T. Kanno, and K. Ono. 1993. Carbamylcholine-induced morphological changes and spatial dynamics of [Ca²⁺]_i in Harderian glands of guinea pigs: calcium-dependent lipid secretion and contraction of myoepithelial cells. *Cell Tissue Res.* **274**: 1–14.
39. Satoh, Y., K. Ishikawa, Y. Oomori, S. Takeda, and K. Ono. 1992. Secretion mode of the harderian gland of rats after stimulation by cholinergic secretagogues. *Acta Anat. (Basel).* **143**: 7–13.
40. Satoh, Y., T. Saino, and K. Ono. 1990. Effect of carbamylcholine on Harderian gland morphology in rats. *Cell Tissue Res.* **261**: 451–459.
41. Sampath, H., M. T. Flowers, X. Liu, C. M. Paton, R. Sullivan, K. Chu, M. Zhao, and J. M. Ntambi. 2009. Skin-specific deletion of stearoyl-CoA desaturase-1 alters skin lipid composition and protects mice from high fat diet-induced obesity. *J. Biol. Chem.* **284**: 19961–19973.
42. Harlow, H. J. 1984. The influence of Harderian gland removal and fur lipid removal on heat loss, and water flux to and from the skin of muskrats, *Ondatra zibethicus*. *Physiol. Zool.* **57**: 349–356.
43. Knudsen, J., P. Hojrup, H. O. Hansen, H. F. Hansen, and P. Roepstorff. 1989. Acyl-CoA-binding protein in the rat. Purification, binding characteristics, tissue concentrations and amino acid sequence. *Biochem. J.* **262**: 513–519.
44. Watanabe, M. 1980. An autoradiographic, biochemical, and morphological study of the harderian gland of the mouse. *J. Morphol.* **163**: 349–365.